Product polarization and mechanism of Li + HF ($v = 0$, $j = 0$) $\rightarrow$ LiF (v', j') + H collision reaction*

Yue Xian-Fang(岳现房)†

Department of Physics and Information Engineering, Jining University, Jining 273155, *China*

(Received 26 March 2013; revised manuscript received 28 May 2013)

A state-to-state dynamics analysis for the Li + HF ($v = 0$, $j = 0$) $\rightarrow$ LiF (v', j') + H collision reaction has been performed through quasiclassical trajectory (QCT) calculations. It is found that the differential cross section (DCS) of the LiF products from the title reaction is preferentially backward scattering for v'=0, yet forward scattering for v'=1 and 2. For v'=3, the DCS exhibits forward, backward, and sideways scatterings. The variation of the internuclear distances and angles along the propagation time reveals that more than 99.08% of reaction trajectories undergo the direct reaction mechanism. The values of the polarization parameters $a_{1-}^{\{1\}}$ and $a_0^{\{2\}}$ demonstrate that the product rotational angular moment $\boldsymbol{j}'$ is not only aligned perpendicular to the reagent relative velocity vector $\boldsymbol{k}$, but also oriented along the negative y axis. These product polarization results agree well with the recent quantum mechanical studies. The mechanism of these results was proposed and discussed in detail.

Keywords: product polarization, collision reaction, state-to-state resolved differential cross section, quasiclassical trajectory

PACS: 34.50.Pi, 34.50.Lf, 82.20.Bc **DOI:** 10.1088/1674-1056/22/11/113401

1. Introduction

After the pioneering work of Taylor and Datz,[1] a large number of experimental and theoretical studies on reactions between the alkali metal atoms (M) and hydrogen halide molecules (HX) have been performed in the past decades. The Li + HF $\rightarrow$ LiF + H reaction, as the lightest member of the MHX system, has manifested rich and complex dynamics because its potential energy surface (PES) involves characteristics of the late barrier, bent transition state structure, as well as the covalent/ionic curve crossing. Much attention has been paid to the reaction dynamics of LiFH system in experiment[2–9] and theory.[10–42]

Experimentally, Becker *et al.*[2] carried out the first crossed molecular beam (CMB) study on the Li + HF $\rightarrow$ LiF + H reaction. They found that the differential cross section (DCS) was nearly a forward–backward symmetry at the collision energy (E_c) of 130 meV, while a strongly forward peaked distribution at E_c = 377 meV. The different DCSs were attributed to a change in the reaction mechanism from the formation of a long lived complex at the low collision energy of 130 meV to a direct process at the high collision energy of 377 meV.[2] Loesch and co-workers[3–7] performed a lot of CMB experiments on the influence of reagent alignment,[3] translational energy,[4,5] vibrational,[3,6] and rotational excitations[7] on the Li + HF $\rightarrow$ LiF + H reaction. In their studies, the alignment of the reagent HF internuclear axis was achieved by changing the direction of the guiding field. The product angular distributions, the partition of available energy, and the integral reaction cross sections (ICSs) showed a marked difference for three different alignments of the HF internuclear axis (namely an isotropic distribution and two others with the molecular axis preferentially aligned along and perpendicular to the relative velocity vector of reagents). Recently, Bobbenkamp *et al.*[5] implemented the effect of the excitation function (collision energy) on the ICS for the Li + HF $\rightarrow$ LiF + H reaction using a new CMB apparatus. A monotonous rise of the excitation function was found with the increase in energies ranging from 25 meV to 131 meV. This predicates that a possible translational energy threshold to the title reaction was significantly smaller than 25 meV, which supported the recent quantum mechanics (QM) studied by Zanchet *et al.*[8] who have found a threshold of $\sim$ 10 meV. Hudson *et al.*[9] observed the van der Waals complex Li$\cdots$FH and probed the dynamics of the excited-state reaction, Li*(2p ^{2}P) + HF $\rightarrow$ LiF + H, by varying the excitation wavelength ranging from 570 nm to 970 nm while recording the photodepletion of the complex.

Theoretically, a series of semi-empirical[10–12] and *ab initio* potential energy surfaces (PESs)[13–21] have been developed for the LiFH system. Employing these PESs, a great amount of quasiclassical trajectory (QCT),[6,7,22–25] time independent quantum mechanics,[26–31] and time dependent wave packet calculations have been performed for the Li + HF reaction.[29–39] Paniagua *et al.*[40–42] studied the transition state spectroscopy via infrared excitation of the Li$\cdots$HF

*Project supported by the National Natural Science Foundation of China (Grant No. 21003062) and the Foundation for Outstanding Yong Scientist of Shandong Province, China (Grant No. BS2012SF002).

†Corresponding author. E-mail: xfyuejnu@gmail.com

© 2013 Chinese Physical Society and IOP Publishing Ltd

and Li···DF complex. Correspondingly, effects of the PES on spectroscopy of the transition state were also investigated by Burcl *et al.*[42] Recently, Zanchet *et al.*[8] obtained the exact quantum state-to-state DCSs of the title reaction at E_c = 97 meV, 136 meV, and 241 meV by using the wave packet method. Later, González-Sánchez *et al.*[39] investigated the influence of reactants? polarization on the DCS of the Li + HF$(v,\ j,\ m) \rightarrow$ LiF$(v',\ j',\ m')$ + H reactions with the same method. It was found that the reactivity is enhanced for nearly collinear collisions. The LiF$(v' = 0)$ products are preferentially forward scattered, while vibrationally excited LiF$(v' = 1$ and 2) are backward scattered. Their results were attributed to the characteristics of the later barrier, bent geometry of the transition state, and a covalent/ionic curve crossing. Most of these investigations have verified that the title reaction contains rich and complex dynamics, and hence further studies on reaction mechanisms are necessary to elucidate the dynamics of the Li + HF reaction.

In the present work, we carried out the QCT calculations on the Li + HF$(v = 0,\ j = 0) \rightarrow$ LiF$(v',\ j')$ + H reaction at E_c = 363 meV. The product state resolved DCSs, the first real polarization parameters, the product rovibrational state distributions, as well as the variations of three internuclear distances and bond angles along the propagation time were computed and presented. A possible reaction mechanism was proposed in terms of the direct interaction with product repulsion (DIPR) mode,[43] which has rationally interpreted most of our calculated results.

2. Theory

A latest *ab initio* PES for the ground state (1^2A') of the LiFH system has been used in our calculations. This PES was developed by Aguado, Paniagua, and Werner (also called APW PES in the literature), which has been used in recent studies.[5,7,8] The energies and geometries of the reaction barrier and well in this PES are in reasonable agreement with the previous ones in the Laganà *et al.* PES[15] and Aguado *et al.* PES.[17,18] The barrier height of the APW PES, 0.221 eV, is higher than that of the Laganà *et al.* PES (0.182 eV),[15] while slightly smaller than that of the Aguado *et al.* PES (0.233 eV).[18] In the entrance channel, the complex well of the APW PES is −0.243 eV, which is shallower than that of the Aguado *et al.* PES (−0.279 eV)[18] or the Laganà *et al.* PES (−0.302 eV).[15] Considering the zero-point energy effect, the exoergicity of the Li + HF$(v = 0,\ j = 0) \rightarrow$ LiF$(v' = 0,\ j' = 0)$ + H reaction on the APW PES is $\Delta H_0^0 = -0.080$ eV, which is slightly larger than that on the Laganà *et al.* PES ($\Delta H_0^0 = -0.040$ eV),[15] However, it is slightly smaller than that on the Aguado *et al.* PES ($\Delta H_0^0 = -0.116$ eV).[18] Figure 1 shows some features of the APW PES.

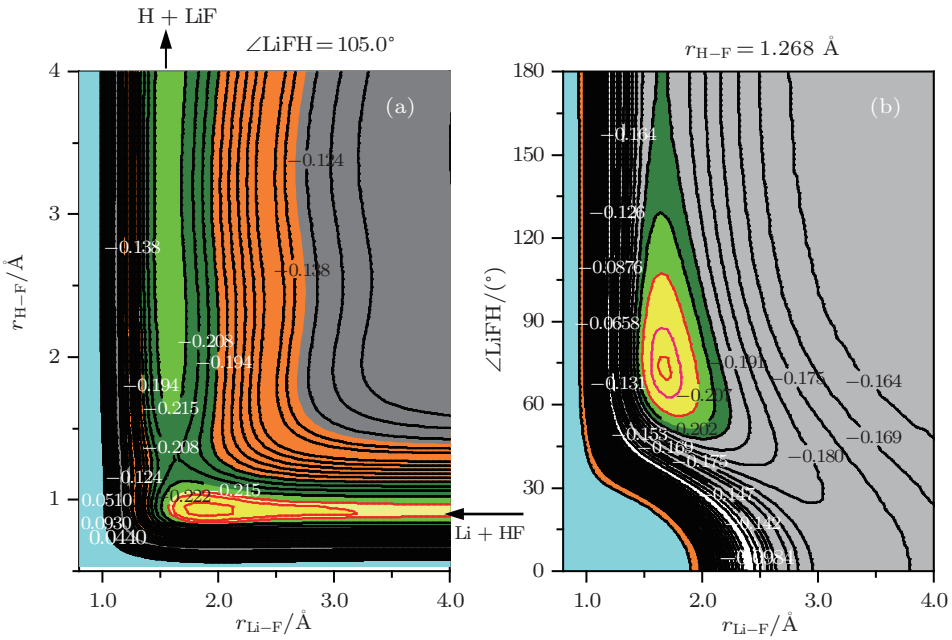


Fig. 1. (color online) Two-dimensional cuts of the PES for configurations of the deep well in the entrance channel at ∠LiFH = 105.0° (a) and the saddle point at r_{HF} = 1.268 Å (b).

The QCT methodology used in the present study is the same as that in Refs. [44]–[51]. At the collision energy of 363 meV, batches of 1×10^5-trajectories have been calculated on the APW PES for the title reaction. With the sixth order gradient symplectic integrator method,[47] an integration step of 0.1-fs ensured a conservation of total energy and total angular momentum better than 10^{-5} and 10^{-7}, respectively. Since the potential has long range forces in both the entrance and the exit channels, the trajectories are started and finished at a distance of 15.0 Å between the Li atom and the CM of the

HF molecule. The value of the maximum impact parameter, $b_{\max}$, is 1.787 Å. The value of b is selected by $b = \beta^{1/2} b_{\max}$, where β is a random number in the [0, 1] region. The orientation of the diatomic molecule, the phase of the diatomic vibrational motion, and β are randomly sampled by using the Monte Carlo method. The vibrational and rotational levels of the reagent molecule are taken as $v = 0$ and $j = 0$, respectively. The atom mass is chosen to be 6.941 a.u. (atomic units) for Li, 18.9984 a.u. for F, and 1.008 a.u. for H, respectively.

The center-of-mass (CM) coordinate was used as the reference coordinate in the present study, which is depicted in Fig. 2. The reagent relative velocity vector $\boldsymbol{k}$ is parallel to the z axis. The x–z plane is the scattering plane which contains the initial and final relative velocity vectors, $\boldsymbol{k}$ and $\boldsymbol{k}'$. The θ_t is the angle between the reagent relative velocity and the product relative velocity (so-called scattering angle), θ_r and φ_r are the polar and azimuthal angles of the final rotational angular momentum $\boldsymbol{j}'$.

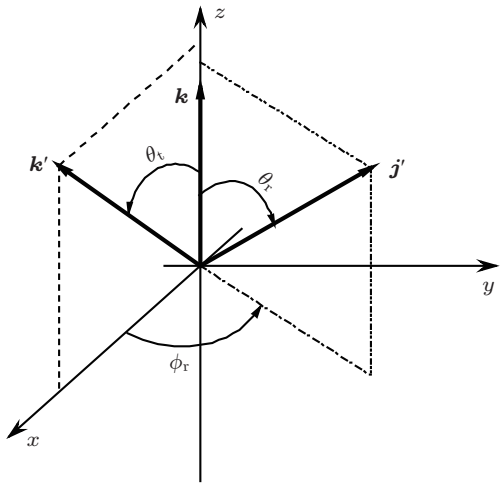


Fig. 2. Center-of-mass coordinate system used to describe $\boldsymbol{k}$, $\boldsymbol{k}'$, and $\boldsymbol{j}'$ correlations.

The differential cross section, $\mathrm{d}\sigma_r/\mathrm{d}\omega$, is calculated by using the method of moments expansion in Legendre polynomials[45,46]

$$\frac{\mathrm{d}\sigma_r}{\mathrm{d}\omega} = \frac{\sigma_r}{2\pi}\left[\frac{1}{2} + \sum_{n=1} a_n \mathrm{P}_n(\cos\theta_t)\right], \tag{1}$$

where the coefficients are given by

$$a_n = \frac{2n+1}{2}\langle \mathrm{P}_n(\cos\theta_t)\rangle = \frac{2n+1}{2}\frac{1}{N_r}\sum_{i=1}^{N_r} \mathrm{P}_n(\cos\theta_{t_i}). \tag{2}$$

Here, σ_r ($= \pi b_{\max}^2 N_r/N_{tot} = 0.305$ Å) is the total integral reactive cross section. The angular brackets represent the Monte Carlo average over the total number of reactive trajectories, N_r, N_{tot} is the total number of trajectories. A good convergence was achieved for the DCS when using the first seven Legendre moments in Eq. (1).

In order to describe the polarization degree of the product rotational angular momentum $\boldsymbol{j}'$, the first real polarization parameters (PPs) $a_{1-}^{\{1\}}$ and $a_0^{\{2\}}$ [52] are calculated, whose expressions are

$$a_{1-}^{\{1\}} = \langle \sin\theta_j \sin\varphi_j\rangle = \langle j'_y/j'\rangle, \tag{3}$$

$$a_0^{\{2\}} = \left\langle 3\cos^2\theta_j - 1\right\rangle = \left\langle 3\frac{j'^2_z}{j'^2} - 1\right\rangle, \tag{4}$$

where j'_y and j'_z are the components of $\boldsymbol{j}'$ along the y and z axes, respectively. The angle $\theta_j = \theta_r$, and $\varphi_j = \varphi_r$. The $a_{1-}^{\{1\}}$ contains information on the orientation of the final rotational angular momentum $\boldsymbol{j}'$, while the $a_0^{\{2\}}$ reflects the alignment of the $\boldsymbol{j}'$.

3. Results and discussion

The total and vibrationally state resolved DCSs of the LiF products from the Li + HF ($v = 0$, $j = 0$) → LiF ($v' = 0$–3, j') + H reaction are shown in Fig. 3. As displayed in Fig. 3(a), the DCS distribution for v'=0 exhibits a large broad peak in the backward direction ($\theta_t = 180°$), while a medium one in the forward direction ($\theta_t = 0°$). This indicates that the product DCS for $v' = 0$ is preferentially scattered backwards. In contrast with the DCS distribution for $v' = 0$, the DCSs for $v' = 1$ and 2 show sharp large peaks in the forward direction, while a moderate (Fig. 3(b)) or a small peak (Fig. 3(c)) in the backward direction. Several tiny peaks in the sideways direction were also observed for the DCSs in Figs. 3(b) and 3(c). For $v' = 3$, the DCS shows a complex distribution that has a large peak in the forward direction, a moderate peak in the backward direction, and a medium peak in the sideways direction. Characteristics of these vibrationally resolved DCSs reveal that the title reaction undergoes the mainly direct reaction mechanism. Figure 3(e) presents the total DCS of the Li + HF ($v = 0$, $j = 0$) → LiF ($v' = 0$–3, j') + H reaction. Obviously, our results are in good agreement with the previous ones calculated by Bobbenkamp *et al.*[7] under the same PES and collision energy. Note that the DCS of the LiF products for $v' = 0$ is much larger than that for $v' = 1$–3, implying that most of the LiF products are in the ground vibrational state. Figure 3(f) provides the product vibrational state distributions for the title reaction. Evidently, about 65.71 percent of the LiF products exist in the ground vibrational state. The remaining are in the vibrationally excited states $v' = 1$, 2, and 3. In 2009, Roncero's group[7] obtained the vibrationally state resolved DCSs of the Li + HF ($v = 0$, $j = 0$) → LiF ($v' = 0$–2, j') + H reaction at $E_c = 241$ meV by using a wave packet method. They found that the DCS prefers forward scattering for $v' = 0$, backward scattering for $v' = 1$, and sideways scattering for $v' = 2$. Very recently, They[39] investigated the role of reactants polarization on the DCS for the state-to-state Li

+ HF (v, j, m) → LiF (v', j', Ω') + H reaction. At the collision energies of E_c = 110 meV, 203 meV, and 317 meV, they calculated the vibrationally state resolved DCSs of the LiF products from the Li + HF ($v = 0$, j = 1–3) → LiF (v' = 0–2, j') + H reactions. It was found that the LiF ($v' = 0$) products were preferentially forward scattered, while the vibrationally excited LiF (v' = 1 and 2) were backward scattered. Unfortunately, our vibrationally state resolved DCSs showed contrary behaviors compared with Roncero's QM ones. For the $v' = 0$, our QCT DCS displays preferentially backward scattering, while underlying forward scattering for the QM one. For v' = 1 and 2, the QM DCSs demonstrate preferentially backward scattering, while underlying forward scattering for our QCT one. However, similar behavior was found for the total DCS, namely, both the QM and QCT DCSs are forward and backward scattered. These differences were attributed to the excitation function (collision energy) or the quantum effects, such as the transition state resonances.[8,39]

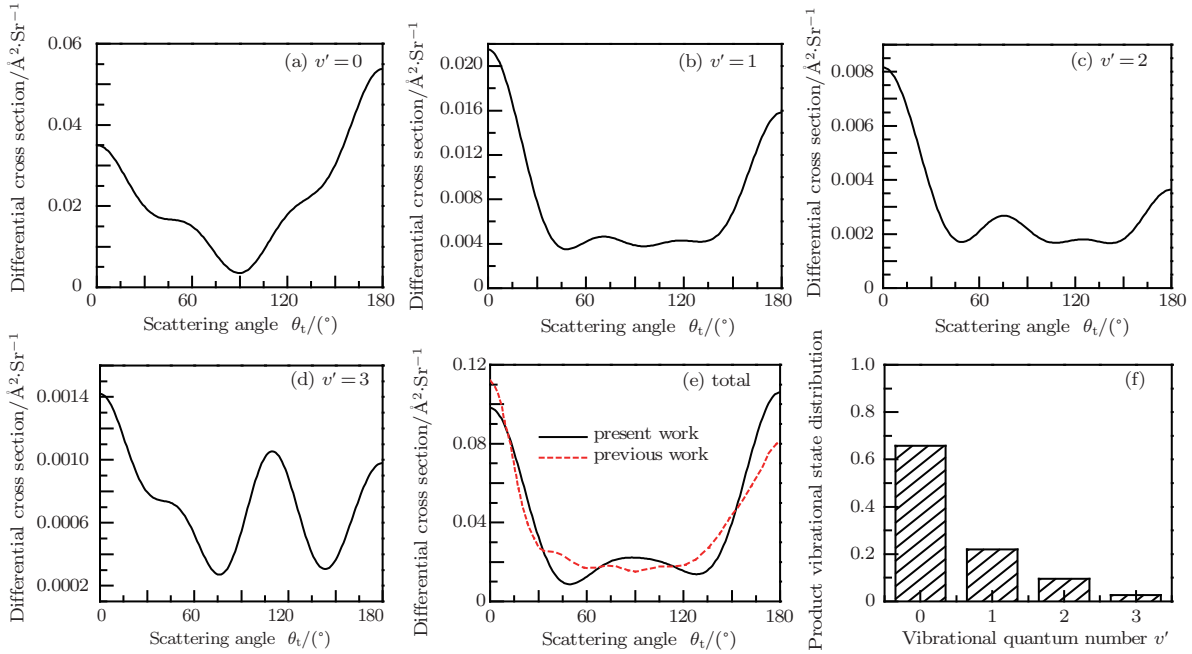


Fig. 3. (color online) (a)–(d) The vibrationally resolved DCSs of the LiF products from the Li + HF ($v = 0$, $j = 0$) → LiF (v', j') + H reaction. (e) Comparison of the total DCS between our present calculated results and the previous QCT results in Ref. [7]. (f) Product vibrational state distribution as a function of the vibrational quantum number v'.

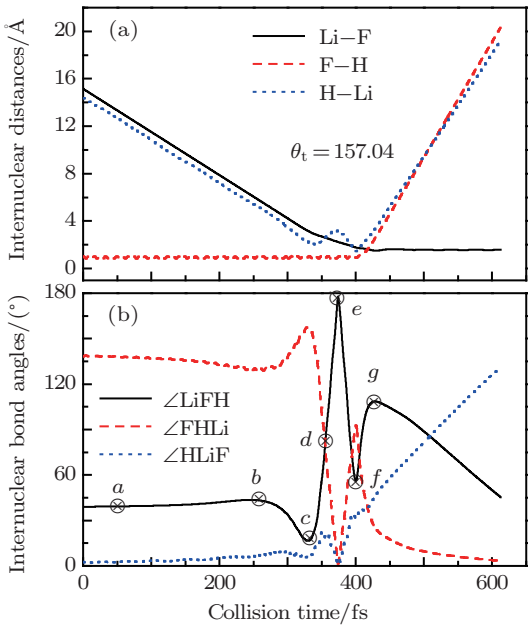


Fig. 4. (color online) Variations of three internuclear distances (a) and bond angles (b) with propagation time.

In order to penetrate into the reaction mechanism of the title reaction, we have observed the evolutionary trajectories of numerous reactive collision processes with the propagation time. Figure 4 plots variations of three internuclear distances of the Li–F, F–H, and H–Li, as well as three internuclear bond angles of the ∠LiFH, ∠FHLi, and ∠HLiF as functions of the propagation time. It was found that most of the reactive trajectories undergo a short collision time ($\lesssim$ 900 fs), the same as the process demonstrated in Fig. 4(a). As an example, figure 4(a) displays the evolution of three internuclear distances for one typical reactive trajectory, which shows that the Li atom collides with the HF molecule and forms the LiF product that moves away immediately. Therefore, the reactive collisions experienced the direct reaction mechanism. According to the statistical analysis, the mechanism of at least 99.08% of the total reactive trajectories are direct reaction.

As shown in Fig. 4(b), the attacking angle of ∠FHLi is initially about 136°. It was found that, for almost all of the reactive trajectories, the initial attacking angle of ∠FHLi ranges

from ∼110° to ∼170°, yet the ∠HLiF is close to 0°. With the collision time propagating, a nearly collinear configuration of Li···H − F is formed. That means only from the H-end of the HF molecule with a large angle of ∠FHLi does the Li atom attack the HF molecule and the title reaction could occur. This observation is coincident with the previous QM[8,39] and QCT[7] results. According to "Polanyi rules", the vibrational energy is more efficient than the translational energy in activating a late barrier reaction, whereas the reverse is true for an early barrier. The Li + HF reaction has a late barrier. The head-end attack from the Li atom to the H-end of the HF molecule favors the target molecule vibration, thus the reaction becomes advantageous. Therefore, the preference for reactions with the head-end collisions is ascribed to the late barrier.

The reaction mechanism can also be reflected by the opacity function of $P(b)$ depicted in Fig. 5. Apparently, the title reaction is more favorable in small impact parameter collisions, which is the feature of the direct reaction mechanism. Figure 6 shows the product rotational state distributions of the Li + HF ($v = 0$, $j = 0$) → LiF ($v' = 0$–3, j') + H reaction. Obviously, the rotational state distributions are inverted for each of the vibrational states, and highly excited up to $j' = 46$ for $v' = 0$, $j' = 43$ for $v' = 1$, $j' = 35$ for $v' = 2$, and $j' = 29$ for $v' = 3$. Figure 7(a) shows the values of the $a_{1-}^{\{1\}}$ as a function of the rotational quantum number j'. Obviously, most of the $a_{1-}^{\{1\}}$ values are negative. As defined in Eq. (3), $a_{1-}^{\{1\}}$ ($=\langle \sin\theta_j \sin\varphi_j \rangle$) contains information on the orientation of $\boldsymbol{j}'$ along the y axis. Its minimum value is −1 and corresponds to the situation that $\boldsymbol{j}'$ orientate along the negative y axis. Correspondingly, the maximum value is +1, indicating that $\boldsymbol{j}'$ preferentially orientate along the positive y axis. Because the range of θ_j is $0° \le \theta_j \le 180°$, $\sin\theta_j$ is greater than or equal to 0. Here, the values of $a_{1-}^{\{1\}}$ are negative, therefore, $\sin\varphi_j$ should be negative, meaning that the range of φ_j is $180° < \varphi_j < 360°$ and implying that the orientation of the product rotational angular momentum $\boldsymbol{j}'$ points to the hemisphere along the negative y axis. At large rotational quantum number j', the values of $a_{1-}^{\{1\}}$ are close to −1, meaning that the orientation of $\boldsymbol{j}'$ aligns primarily along the negative y axis. The statistical average value of $a_{1-}^{\{1\}}$ is −0.84 over all the products, suggesting that the orientation of the product rotational angular momentum $\boldsymbol{j}'$ is preferentially along the negative y axis. The bottom panel of Fig. 7 displays the values of the alignment parameter $a_0^{\{2\}}$ for the LiF products. As expressed in Eq. (4), the value of the $a_0^{\{2\}}$ equals to −1 when $\theta_j = 90°$, and at this moment the alignment of $\boldsymbol{j}'$ is exactly perpendicular to the $\boldsymbol{k}$. For the Li + HF ($v = 0$, $j = 0$) → LiF (v', j') + H reaction, almost all $a_0^{\{2\}}$ values are negative, and they approach to −1 for the products with the large rotation quantum number j'. The statistical average value of $a_0^{\{2\}}$ for all the products is −0.93, which means that alignment of the product rotational angular momentum $\boldsymbol{j}'$ is preferentially along the direction perpendicular to the $\boldsymbol{k}$. Our results are in excellent agreement with the recent QM results obtained by González–Sánchez *et al.*,[39] in which the calculated alignment was close to −1. That means that the product rotational angular momentum is not only preferentially aligned perpendicular to the $\boldsymbol{k}$, but also its underlying orientation is to the negative y axis.

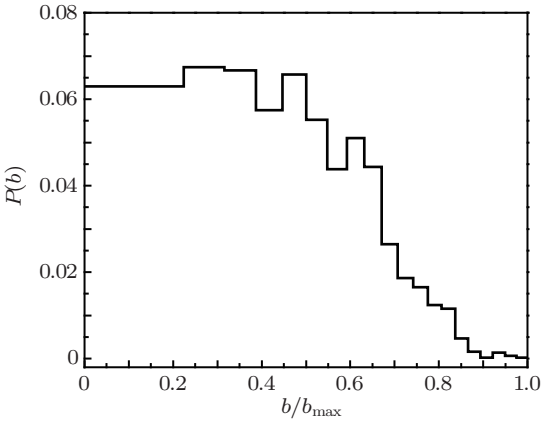


Fig. 5. Reactive probability as a function of the impact parameter (opacity function).

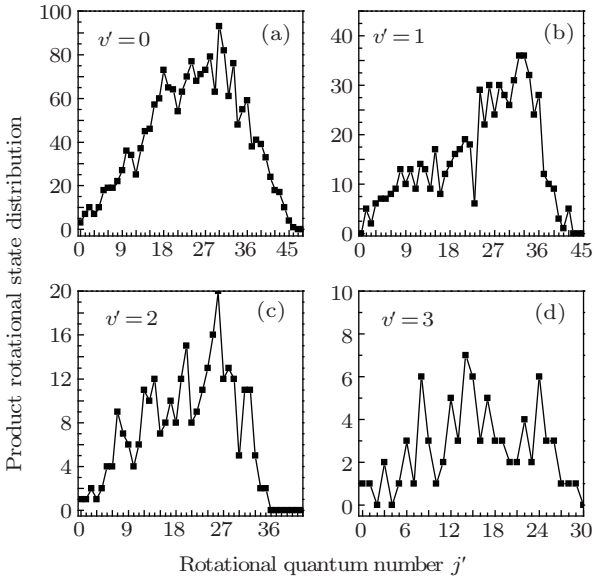


Fig. 6. Product rotational state distributions as functions of the rotational quantum number j'. (a) $v' = 0$, (b) $v' = 1$, (c) $v' = 2$, (d) $v' = 3$.

For reactions involving alkali metal atoms, the reaction mechanism has been regularly interpreted by the direct interaction with product repulsion (DIPR) mode proposed originally by Kuntz and co-workers.[53,54] As a representative reaction between alkali metal atoms and hydrogen halide molecules, the reactive collision process could be rationally explicated by using the DIPR mode. Combining the evolution of the reactive trajectory and the DIPR mode shown in Figs. 4 and 8, we present a cartoon to describe the reaction mechanism for the title reaction. Initially, the Li atom approaches the H-end of the HF molecule with a large angle of ∠FHLi and long distance between the Li atom and the CM of the HF

molecule (displayed in Fig. 8(a)). As the Li atom approaches, the Li atom would impel the H atom to close the F atom, and therefore the HF molecule is evoked to vibrate. The vibration of the reagent HF significantly facilitates the reaction to occur in the light of "Polanyi rules". This can explain why the title reaction favors the head-end collision reaction. Under the mutual interaction of the relative reagent velocity and van der Waals forces, the Li atom will arrive at the F-end of the HF molecule displayed in Fig. 8(d) via intermediate configurations the same as those shown in Figs. 8(b) and 8(c), respectively. Under the molecule configuration of Fig. 8(d), an electron of the Li atom "jumps" to the F atom, and hence the ionic electronic state of the HLi^+F^- system is formed. Coulomb force between the Li^+ and F^- rapidly shortens the internuclear distance of the LiF. On the ionic electronic PES, the Li atom comes back to the bent geometry of the saddle point depicted in Fig. 8(e). At the saddle point, the curve crossing occurs between the covalent and ionic electronic states, and then the LiFH system gets into its exit channel of LiF + H. Subunit of the HF^- has a strong repulsive potential curve (depicted in Fig. 8(f)), which impels the H atom to depart quickly from the HLi^+F^- system and pushes the F^- to move. As described in Fig. 8(g), the repulsive energy of the HF^- leads to rotationally excited Li^+F^- products and forward scattering. During the reactive encounter, the total angular momentum is conserved, i.e., $\boldsymbol{J} = \boldsymbol{L} + \boldsymbol{j} = \boldsymbol{L}' + \boldsymbol{j}'$, where $\boldsymbol{J}$ is the total angular momentum, $\boldsymbol{L}$ and $\boldsymbol{L}'$ are the reagent and product orbital momenta, respectively, $\boldsymbol{j}$ is the reagent rotational angular momentum, and here it is zero because the reagent rotational quantum number j of the HF molecule is zero. Accordingly, the conservation of angular momentum becomes $\boldsymbol{L} = \boldsymbol{L}' + \boldsymbol{j}'$. Since $\boldsymbol{L}$ and $\boldsymbol{L}$' are perpendicular to $\boldsymbol{k}$ and $\boldsymbol{k}$', respectively, both of them are perpendicular to the scattering plane. Therefore, the product rotational angular momentum $\boldsymbol{j}'$ is perpendicular to the scattering plane, thus it is perpendicular to the $\boldsymbol{k}$. This provides the reason why the average alignment value of $\boldsymbol{j}'$ is close to -1. Because the H atom is very light, its departing results in small angular momentum $\boldsymbol{L}$'. The angular momentum conservation can be approximately expressed by $\boldsymbol{L} \approx \boldsymbol{j}'$. Consequently, not only the value but also the direction of the product rotational angular momentum $\boldsymbol{j}'$ is close to the total angular momentum $\boldsymbol{J}$. These inferences could interpret the results that the product rotational state is highly excited, and the orientation of the $\boldsymbol{j}'$ is along the negative y axis.

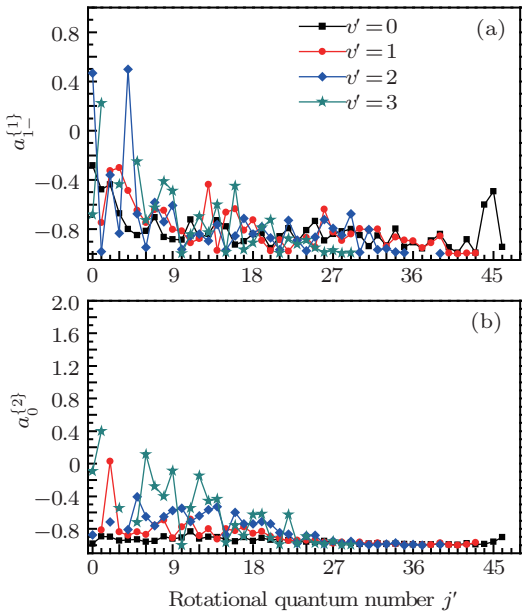


Fig. 7. (color online) Values of the first real polarization parameters of $a_{1-}^{\{1\}}$ (a) and $a_0^{\{2\}}$ (b) as a function of the rotational quantum number j'.

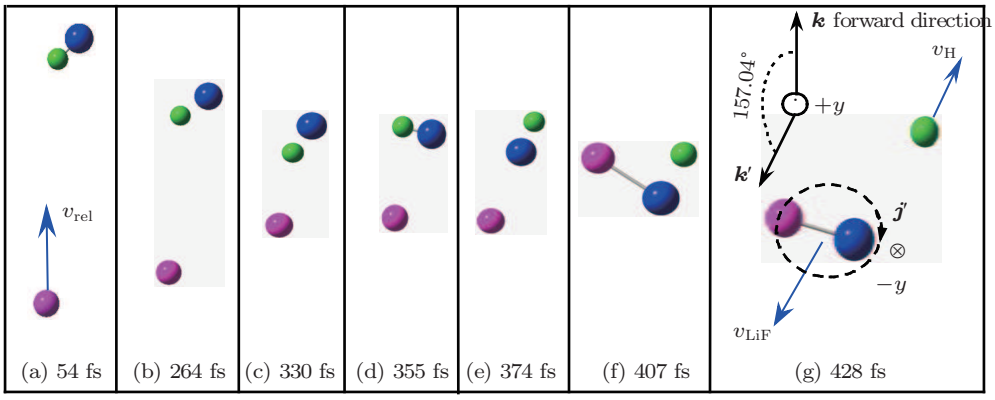


Fig. 8. (color online) Configurations of the LiHF system at the propagation time of (a) 54 fs, (b) 264 fs, (c) 330 fs, (d) 355 fs, (e) 374 fs, (f) 407 fs, and (g) 428 fs. Panel (g) illustrates the direct reaction mechanism of the title reaction.

4. Conclusion

In the present work, we carried out the QCT calculations on the Li + HF ($v = 0$, $j = 0$) $\rightarrow$ LiF (v', j') + H reaction under the latest PES and $E_c = 363$ meV. The vibrational state resolved differential cross sections, product state distributions, evolutionary trajectories over the propagation time, as well as the first real polarization parameters are presented and analyzed. It was found that the vibrational state resolved DCSs are preferentially forward scattered for both the vibrational states

of $v' = 0$ and 1, thereby, the total DCS favors the preferential forward scattering. Analysis of the product state distributions demonstrates that about 65.71% of the LiF products are in the ground vibrational state $v' = 0$, and the rest are in the vibrationally excited states $v' = 1$–3. The rotational state distributions are inverted for each of the vibrational states and highly excited up to $j' = 46$ for $v' = 0$, $j' = 43$ for $v' = 1$, $j' = 35$ for $v' = 2$, and $j' = 43$ for $v' = 3$. The opacity function demonstrates that the smaller the impact parameter is, the higher the reaction probability is. Variations of the internuclear distances and angles reveal that only when from the H-end of the HF molecule with a large angle of ∠FHLi does the Li atom attack the HF, the title reaction could occur. This observation is coincident with the recent QM conclusion of Roncero's group that the title reaction favors the head-on collisions. Analysis of the evolution of reactive trajectories discloses that more than 99.08% of the total reactive events undergo the short collision time (≤ 900 fs), which means that the title reaction is dominantly the direct reaction mechanism. The average values of the first real polarization parameters $a_{1-}^{\{1\}}$ and $a_{0}^{\{2\}}$ are -0.84 and -0.93, respectively, which reveals that the product rotational angular momentum $\boldsymbol{j}'$ is not only aligned perpendicular to the reagent relative velocity vector $\boldsymbol{k}$, but also oriented along the negative y axis. These results are in good agreement with the recent QM ones by Roncero's group. Employing the DIPR model, we presented a cartoon to describe the reaction mechanism and nicely interpreted the calculated results.

References

[1] Taylor E H and Datz S 1955 *J. Chem. Phys.* **23** 1711
[2] Becker C H, Casavecchia P, Tiedemann P W, Valentini J J and Lee Y T 1980 *J. Chem. Phys.* **73** 2833
[3] Loesch H J and Stienkemeier F 1993 *J. Chem. Phys.* **98** 9570
[4] Höbel O, Bobbenkamp R, Paladini A, Russo A and Loesch H J 2004 *Phys. Chem. Chem. Phys.* **6** 2198
[5] Bobbenkamp R, Loesch H J, Mudrich M and Stienkemeier F 2011 *J. Chem. Phys.* **135** 204306
[6] Aoiz F J, Verdasco E, Rábanos V S, Loesch H J, Menéndez M and Stienkemeier F 2000 *Phys. Chem. Chem. Phys.* **2** 541
[7] Bobbenkamp R, Paladini A, Russo A, Loesch H J, Menéndez M, Verdasco E, Aoiz F J and Werner H J 2005 *J. Chem. Phys.* **122** 244304
[8] Zanchet A, Roncero O, González-Lezana T, Rodríguez-López A, Aguado A, Sanz-Sanz C and Gómez-Carrasco S 2009 *J. Phys. Chem. A* **113** 14488
[9] Hudson A J, Oh H B, Polanyi J C and Piecuch P 2000 *J. Chem. Phys.* **113** 9897
[10] Balint-Kurti G G and Yardley R N 1977 *Faraday Discuss. Chem. Soc.* **62** 77
[11] Zeiri Y and Shapxiro M 1978 *Chem. Phys.* **31** 217
[12] Shapiro M and Zeiri Y 1979 *J. Chem. Phys.* **70** 5264
[13] Chen M M L and Schaefer H F 1980 *J. Chem. Phys.* **72** 4376
[14] Carter S and Murrell J N 1980 *Mol. Phys.* **41** 567
[15] Parker G A, Laganà A, Crocchianti S and Pack R T 1995 *J. Chem. Phys.* **102** 1238
[16] Aguado A, Suárez C and Paniagua M 1995 *Chem. Phys.* **201** 107
[17] Aguado A, Paniagua M, Lara M and Roncero O 1997 *J. Chem. Phys.* **106** 1013
[18] Aguado A, Paniagua M, Lara M and Roncero O 1997 *J. Chem. Phys.* **107** 10085
[19] Burcl R, Piecuch P, Špirko V and Bludský O 2000 *Int. J. Quantum Chem.* **80** 916
[20] Jasper A W, Hack M D, Truhlar D G and Piecuch P 2002 *J. Chem. Phys.* **116** 8353
[21] Aguado A, Paniagua M, Sanz C and Roncero O 2003 *J. Chem. Phys.* **119** 10088
[22] Li S J, Shi Y, Xie T X and Jin M X 2012 *Chin. Phys. B* **21** 013401
[23] Tan R S, Liu X G and Hu M 2012 *Chin. Phys. Lett.* **29** 123101
[24] Alvari?no J M, Casavecchia P, Gervasi O and Laganà A 1982 *J. Chem. Phys.* **77** 6341
[25] Jasper A W, Hack M D, Chakraborty A and Truhlar D G 2001 *J. Chem. Phys.* **115** 7945
[26] Parker G A, Laganà A, Crocchianti S and Pack R T 1995 *J. Chem. Phys.* **102** 1238
[27] Wei L, Jasper A W and Truhlar D G 2003 *J. Phys. Chem. A* **107** 7236
[28] Laganà A, Bolloni A and Crocchianti S 2000 *Phys. Chem. Chem. Phys.* **2** 535
[29] Baer M, Last I and Loesch H J 1994 *J. Chem. Phys.* **101** 9648
[30] Skouteris D, Crocchianti S and Laganà A 2007 *Chem. Phys. Lett.* **440** 1
[31] Laganà A, Bolloni A, Crocchianti S and Parker G A 2000 *Chem. Phys. Lett.* **324** 466
[32] Zhu W, Wang D and Zhang J Z H 1997 *Theor. Chem. Acc.* **96** 31
[33] Xie D Q, Li S M and Guo H 2002 *J. Chem. Phys.* **116** 6391
[34] Paniagua M, Aguado A, Lara M and Roncero O 1999 *J. Chem. Phys.* **111** 6712
[35] Lara M, Aguado A, Paniagua M and Roncero O 2000 *J. Chem. Phys.* **113** 1781
[36] Aguado A, Lara M, Paniagua M and Roncero O 2001 *J. Chem. Phys.* **114** 3440
[37] Gómez-Carrasco S and Roncero O 2006 *J. Chem. Phys.* **125** 054102
[38] Sanz C, Roncero O, Paniagua M and Aguado A 2002 *Chem. Phys. Lett.* **351** 295
[39] González-Sánchez L, Vasyutinskii O, Zanchet A, Sanz-Sanz C and Roncero O 2011 *Phys. Chem. Chem. Phys.* **13** 13656
[40] Paniagua M, Aguado A, Lara M and Roncero O 1998 *J. Chem. Phys.* **109** 2971
[41] Paniagua M, Aguado A, Lara M and Roncero O 1999 *J. Chem. Phys.* **111** 6712
[42] Burcl R, Piecuch P, Špirko V and Bludský O 2002 *J. Mol. Struct. Theochem.* **591** 151
[43] Mestdagh J M, Soep B, Gaveau M A and Visticot J P 2003 *Int. Rev. Phys. Chem.* **22** 285
[44] Han K L, He G Z and Lou N Q 1996 *J. Chem. Phys.* **105** 8699
[45] Wang M L, Han K L and He G Z 1998 *J. Phys. Chem. A* **102** 10204
[46] Chen M D, Han K L and Lou N Q 2003 *J. Chem. Phys.* **118** 4463
[47] Zhang X and Han K L 2006 *Int. J. Quant. Chem.* **106** 1815
[48] Li H, Zheng B, Ying J Q and Meng Q T 2011 *Chin. Phys. B* **20** 123401
[49] Liu Y F, He X H, Shi D H and Sun J F 2011 *Chin. Phys. B* **20** 078201
[50] Zhu T, Hu G D, Chen J Z, Liu X G and Zhang Q G 2010 *Chin. Phys. B* **19** 083402
[51] Ge M H and Zheng Y J 2011 *Chin. Phys. B* **20** 083401
[52] Aoiz F J, Brouard M and Enriquez P A 1996 *J. Chem. Phys.* **105** 4964
[53] Kuntz P J, Nemetz E and Polanyi J C 1969 *J. Chem. Phys.* **50** 4607
[54] Kuntz P J, Mok E H and Polany J C 1969 *J. Chem. Phys.* **50** 4623